Electronic Supplementary Material (ESI)

Dye self-organization in doped silica nanoparticles increases the electrochemiluminescence emission in magnetic beads-based assay

Yematawork Addis Alemu, Marinella Difonzo, Damiano Genovese, Francesco Paolucci, Luca Prodi, Enrico Rampazzo, Giovanni Valenti.

Dipartimento di Chimica "Giacomo Ciamician" – Via F. Selmi 2, 40126 Bologna, Italy.

Index

1. Materials. Non-ionic surfactant -Triton™ X-100, tetraethyl orthosilicate (TEOS, 99 %), aqueous ammonia solution (NH_4OH, 28-30 % wt in water), tri-*n*-propylamine (TPrA, ≥98% V/V), sodium phosphate monobasic dihydrate (≥99%), sodium phosphate dibasic (≥99%), sodium carbonate/bicarbonate, hydrochloric acid (HCl, >37%), (3-aminopropyl)triethoxysilane (APTES, ≥98%), 3-(trihydroxysilyl)propyl methyl phosphonate, monosodium salt solution (THPMP, 42% wt in water), reagent grade dimethylformamide (DMF, ≥99.8%,), anhydrous 1-hexanol (≥99%), cyclohexane (≥99.5%), ethanol, acetone and 2-butanone (≥99.0%), *cis*-dichlorobis(2,2′-bipyridine)ruthenium(II) (97%), bathophenanthroline disulfonic acid disodium salt trihydrate ($Na_2BPS \cdot 3H_2O$, 98%), and 2,2′-bipyridine (bpy, ≥ 99%), tris(2,2′-bipyridyl)ruthenium(II) chloride hexahydrate ($Ru(bpy)_3Cl_2.6H_2O$, 99.95%), were purchased from Merck. Biotin-dPEG®$_{12}$-TFP (tetrafluorophenyl) ester (> 98%) was purchased from Quanta Biodesign. Paramagnetic microbeads Dynabeads M-280 Streptavidin (diameter 2.8 µm, 10 mg/mL) were purchased from Thermo Fisher Scientific (Waltham, MA). All reagents and solvents were used as received without further purification. Milli-Q water was used as solvent and washing purposes.

2. Synthesis

$Ru(bpy)_2bps$. This complex was prepared starting from *cis*-dichlorobis(2,2′-bipyridine)ruthenium(II) (97%) and bathophenanthroline disulfonic acid disodium salt trihydrate ($Na_2BPS \cdot 3H_2O$, 98%), and following the experimental procedure reported in Leopoldo Della Ciana et al. *J. Phys. Chem. C* **2010,** *114,* 3653–3658.

Preparation of dye-doped silica NPs with different sizes. DDSNPs were prepared by a reverse microemulsion method adapting previously reported procedures. Briefly, 1.77 g of Triton X-100, 1.6 mL of 1-hexanol and 7.5 mL of cyclohexane were stirred for 10 minutes at 25 °C to produce a single-phase and stable microemulsion (Figure 1-ESI). 60 µL of NH_4OH (28-30 wt %) were added together with a 17 mM aqueous solution of the cationic-$Ru(bpy)_3^{2+}$ or of the zwitterionic $Ru(bpy)_2$bps dye. NPs samples with different sizes were obtained by adding different volumes of the dye solution (270, 370, 980 µL) under stirring and at 25 °C, to achieve a water-to-surfactant molar ratio of 6, 8, and 20 respectively. After 30 minutes, 100 µL TEOS were added, and the reaction proceeded for 24 h. In the second step, another aliquot of TEOS (50 µL) was added followed by the addition of 20 µL of APTES and 30 µL of THPMP, and the microemulsion was stirred for an additional 24 h at 25°C. After this time the NPs were recovered from the microemulsion by treating 1 mL of microemulsion with acetone (~10 mL) and by centrifugation (5000 rpm, 10 min). NPs were washed and centrifugated with acetone three times and finally by ethanol two times. Vortexing and ultrasonication were employed to resuspend the particles after centrifugation. Finally, the NPs were suspended in 1 mL of Milli-Q water and stored at 4°C.

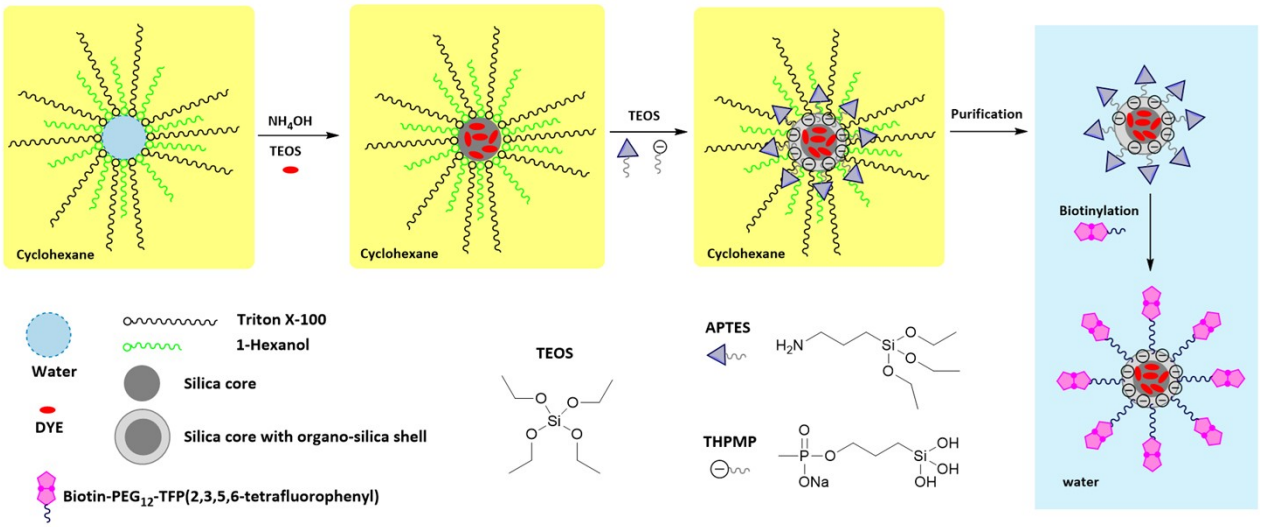

Figure 1-ESI Scheme for the preparation of DDSNPs by reverse microemulsion. The organo-silica shell was formed by the addition of additional TEOS and of APTES (3-aminopropyltriethoxysilane) and THPMP (3-(trihydroxysilyl)propyl methylphosphonate). Biotinylation was performed by reaction of the amine surface groups with biotin-PEG_{12}-TFP active ester.

Biotinylation of DDSNPs. The work-up to collect the NPs was performed on 100 µL of the pristine NPs microemulsion in a 2.0 mL PP vial. The separated NPs were finally dispersed in 100 µL of Milli-Q water and 20 µL of 200 mM carbonate buffer (pH 9.0) were added. After homogenization by vortexing, 15 µL of a 45 mM DMSO solution of Biotin-PEG_{12}-TFP were added, and the suspension was left under orbital stirring at room temperature overnight. The biotinylated NPs were separated and washed by centrifugation after the addition of 1.5 mL of 2-butanone three times and stored in 1 mL Milli-Q water for further conjugation to MMBs.

DDSNPs Conjugation to MMBs. The purified DDSNPs were coupled to MMBs through streptavidin-biotin interactions. Streptavidin-coated MMBs (diameter 2.8 µm, C = 0.7 mg/mL) were left to react with purified biotinylated NPs at 37°C for 3 hours in a Stuart Scientific® thermostatic oven equipped with a rotary shaker. After incubation, the reacted MMBs were washed twice with 200 mM PB buffer and separated from the unreacted NPs by magnetic field. MMBs were finally resuspended in the same buffer, and stored at 4°C (Figure 2-ESI).

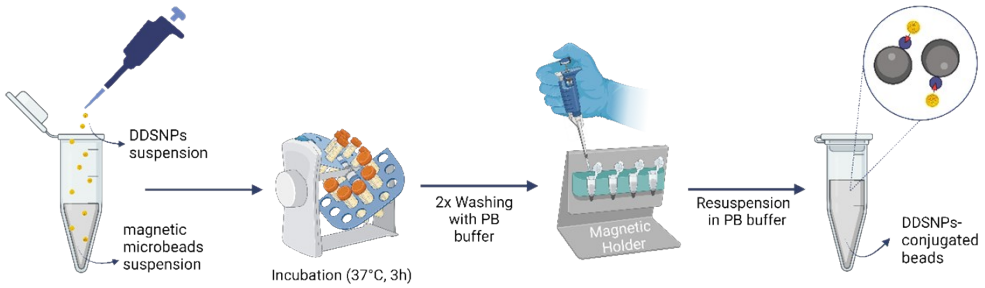

Figure 2-ESI Representation of the procedure for the conjugation of the biotinylated DDSNPs to streptavidin-coated MMBs.

3. Transmission Electron Microscopy (TEM). TEM images were obtained with a Philips CM 100 microscope, operating at 80 kV, and using 3.05 mm copper grids (carbon/Formvar support film, 400 mesh). To prepare the specimen, a small aliquot of DDSNPs suspension in water was diluted 1:50 in an ethanol-water 1:1 mixture. The diluted suspension (4 µL) was dropped on the grid, and after one minute the solvent was removed by a small piece of filtering paper. The grid was then dried under vacuum before the acquisition of TEM images. Image J software was used to perform size analysis on the recorded images (Figure 3-ESI).

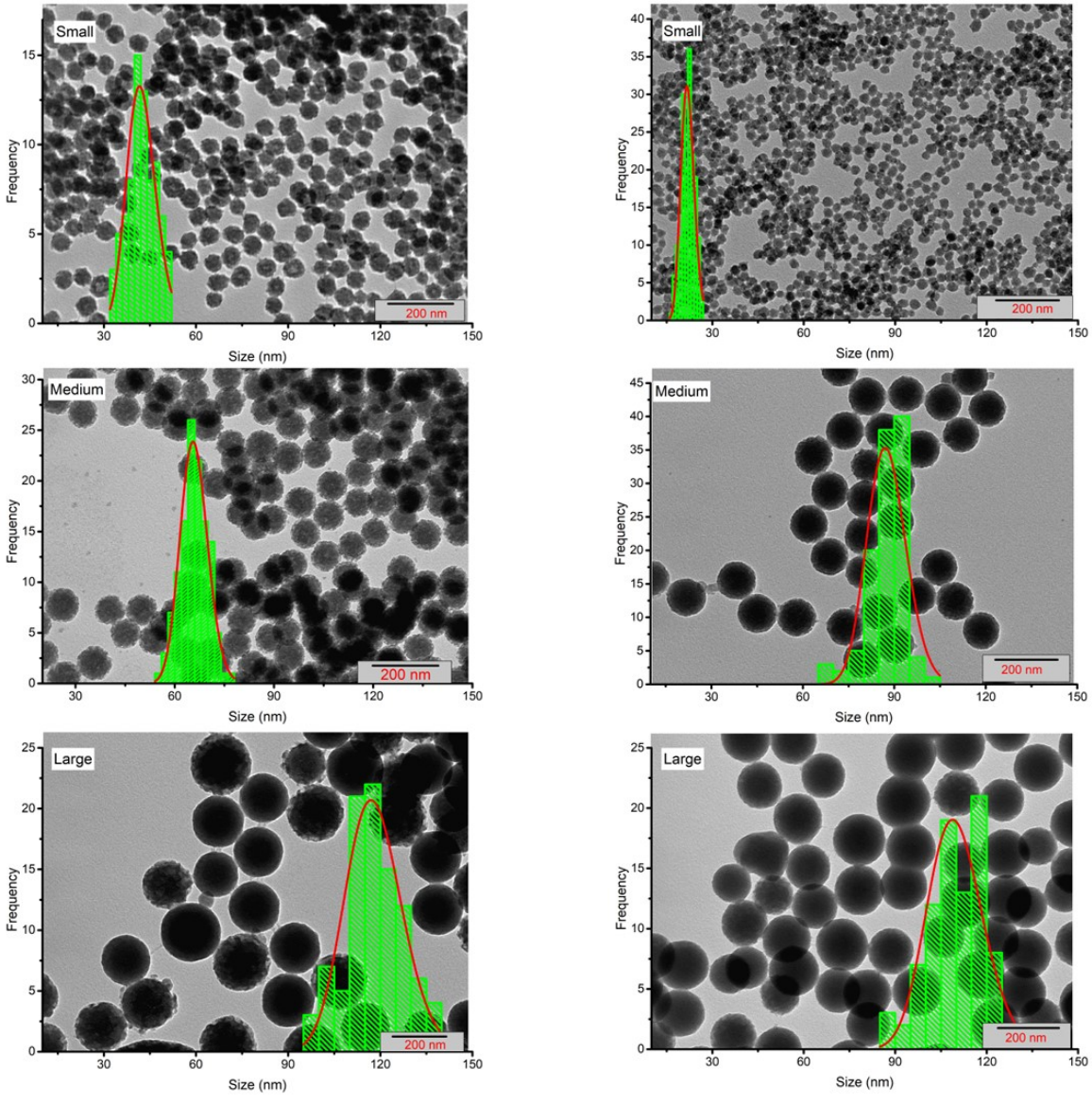

Figure 3-ESI TEM images and silica core diameter distribution for the NPs samples presented in this work.

4. Dynamic Light Scattering (DLS) measurements. Hydrodynamic diameter (d_H) distributions of NPs (Figure 4-ESI and 5-ESI) were obtained in water at 25 °C with a Malvern Nano ZS instrument equipped with a 633 nm laser diode. Suspensions of NPs were prepared with water in PMMA disposable cuvettes of 1 cm optical path length. The width of DLS hydrodynamic diameter distribution is indicated by PDI (Polydispersion Index). In the case of a mono-modal distribution (gaussian) calculated using cumulant analysis, PDI = $(\sigma/ Z_{avg})^2$, where σ is the width of the distribution and Z_{avg} is the average diameter of the NPs population respectively.

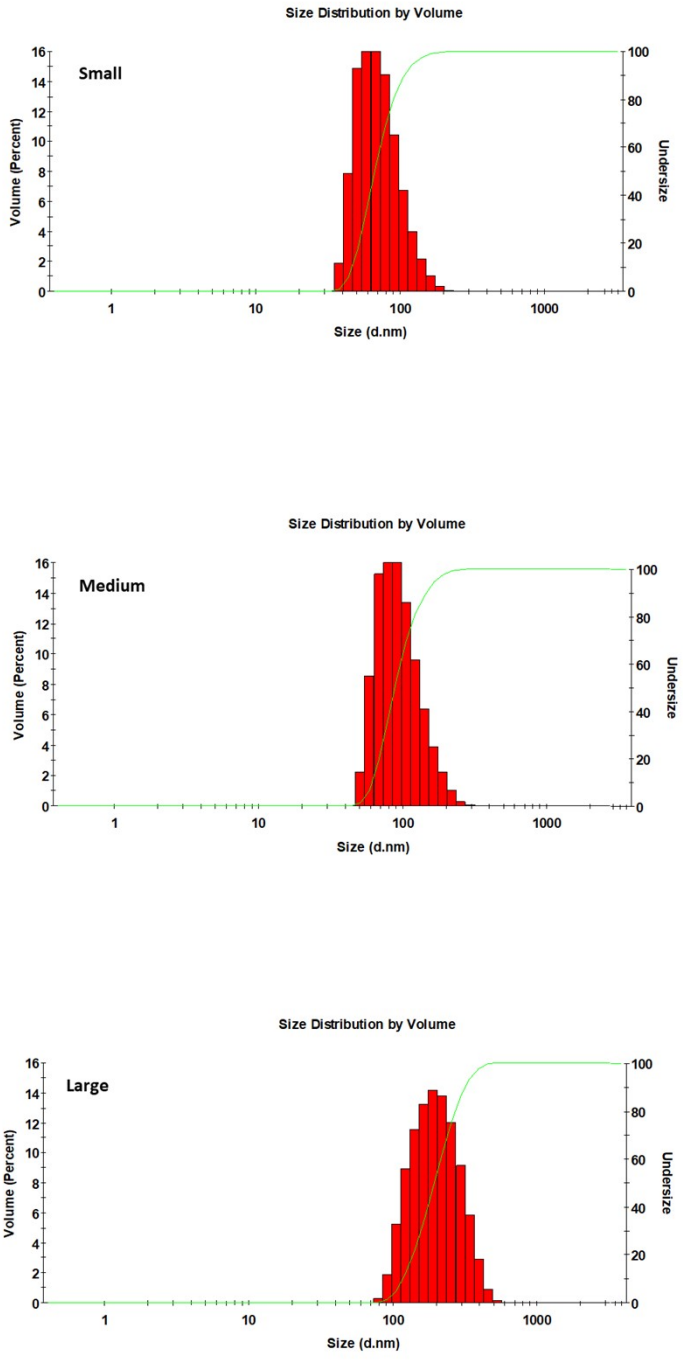

Figure 4-ESI DLS hydrodynamic size distribution for **NPs-Ru(bpy)$_3^{2+}$** (water, 25°C).

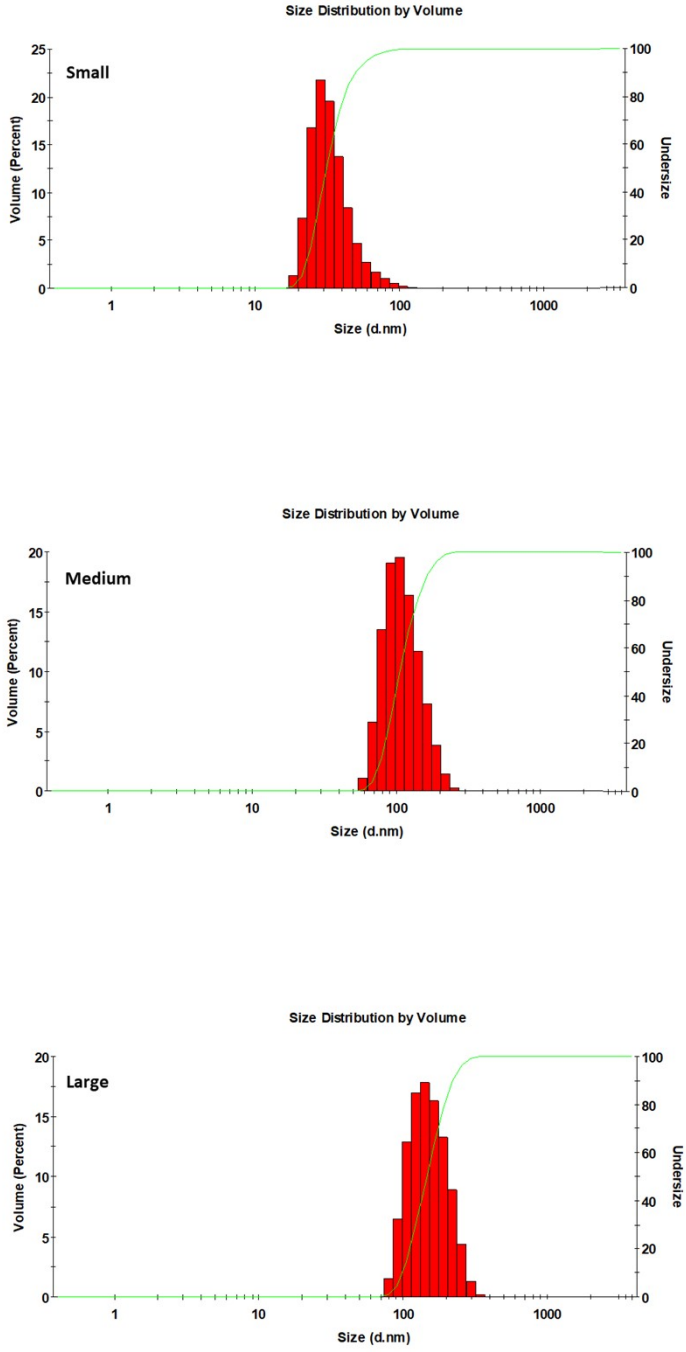

Figure 5-ESI DLS hydrodynamic size distribution for **NPs-Ru(bpy)$_2$bps** (water, 25°C).

5. ζ- Potential. A Malvern Nano ZS instrument equipped with a 633 nm laser source was used. NP dispersions in water were housed in disposable polycarbonate folded capillary cell (DTS1070, 750 µL, 4 mm optical path length). Electrophoretic determination of ζ-potential was made under a Smoluchowski approximation.

6. Photochemical Measurements. Quartz cuvettes with an optical path length of 1 cm were used for both absorbance and emission measurements. UV−Vis absorption spectra were recorded at 25 °C using a PerkinElmer Lambda 45 spectrophotometer, and the luminescence spectra were recorded with a

PerkinElmer Lambda LS 55 fluorometer (Figure 6-ESI). An Edinburgh spectrofluorimeter FLS920 equipped with a photomultiplier Hamamatsu R928P and connected to a PCS900 PC card was used for the time-correlated single photon counting experiments (TCSPC) using an excitation laser at λ = 405 nm. Luminescence quantum yields (ϕ_{PL}) were recorded on air-equilibrated aqueous suspensions using as reference ~~dye~~ an air-equilibrated water solution of the $Ru(bpy)_3^{2+}$ complex (ϕ_{PL} 0.028, ε_{452}(water) 14600 $cm^{-1}M^{-1}$, Handbook of Photochemistry (3rd ed.). CRC Press). The considered molar extinction coefficient in water value for the $Ru(bpy)_2bps$ complex was 18000 $cm^{-1}M^{-1}$ (Leopoldo Della Ciana et al. *J. Phys. Chem. C* **2010,** *114,* 3653–3658).

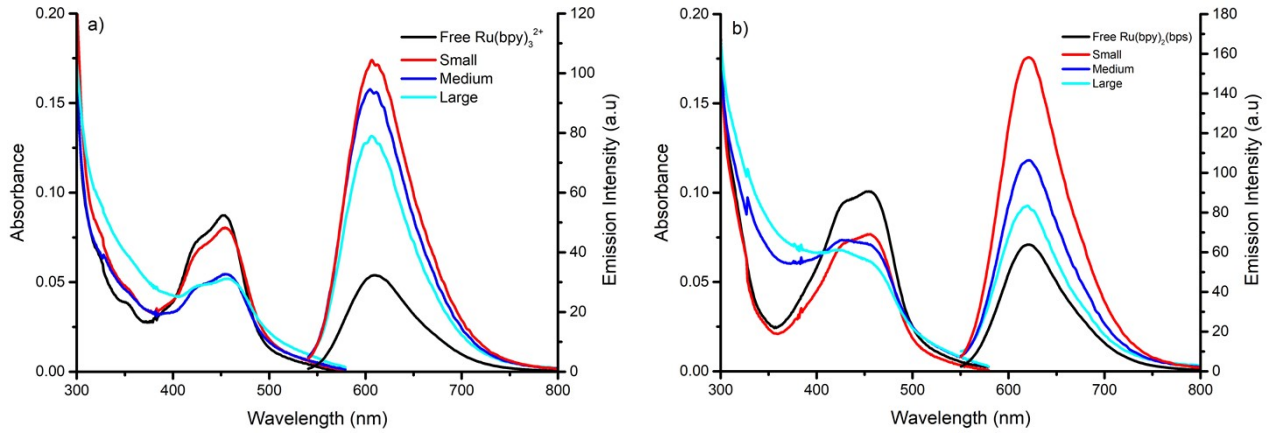

Figure 6-ESI a) Absorption and emission spectra of **NPs-Ru(bpy)$_3^{2+}$** , b) of **NPs-Ru(bpy)$_2$bps** and of their reference dyes $Ru(bpy)_3^{2+}$ and $Ru(bpy)_2bps$ (water, aerated, 25°C, λ_{ex} = 450 nm)

7. Nanoparticles tracking analysis (NTA). A NanoSight NS300 (Malvern, UK) instrument operating in scatter mode (software NTA 3.2 Dev Build 3.2.16) was used for the determination of NPs concentration of the samples NPs- **NPs-Ru(bpy)$_3^{2+}$-large** and **NPs-Ru(bpy)$_2$bps-large.** Before NTA measurements both samples (post work-up concentration) were diluted in water to a final volume of 2 mL (dilution 1:1000) and filtered with a 450 nm RC syringe filter. The following settings according to the Malvern software manual, were used:

Capture Settings: sCMOS camera; Red laser; Camera Level = 16; Slider Shutter = 1300; Slider Gain = 512; FPS = 25.0; Number of Frames: 1498; Temperature: 20.7 - 20.8 °C; Water viscosity = 0.980 - 0.982 cP.
Analysis Settings: Detect Threshold = 5; Blur Size = Auto; Max Jump Distance: Auto = 9.7 - 10.0 pix.

The determination of the concentration of the *medium* and *small* samples by NTA did not provide reliable results, because these samples present a size that is close to or lower than the detection limit (60-70 nm) of the NanoSight NS300 instrument (Daniel Bachurski et al. *J. Extracell. Vesicles* **2019**, *8*, 1596016). However, from the NTA concentration measurements data for the sample **NPs-Ru(bpy)$_3^{2+}$-large** and **NPs-Ru(bpy)$_2$bps -large** and the corresponding average diameter obtained from TEM microscopy, considering an average silica density of 2.0 g/mL (*Mol. Pharmaceutics* **2018**, *15*, 2372), it was possible to verify that the hydrolysis of the TEOS silica precursor in the microemulsion was almost quantitative. Under the assumption that this can be extended to all syntheses, and therefore that the amount of TEOS precursor added in each synthesis of NPs with different sizes is quantitatively converted into an equal total volume of silica, using the TEM diameters for the *small* and *medium* NPs, the concentrations for these samples were calculated via the following simple relationship

$C_i = C_L * V_i / V_L$

Where *C* and *V* are concentration and volume of the nanoparticles, respectively, and *i* and *L* stand for the unknown sample and the large nanoparticles sample (measured experimentally), respectively. The resulting data are presented in Table 1-ESI.

Table 1-ESI Average concentration of NPs samples in water (post work-up concentration) and corresponding number of Ru(II) complexes per NP. a: experimental; b: calculated.

Sample name		No. of NP / ml	No. dye/ NP
NPs-Ru(bpy)$_3^{2+}$	**Large**[a]	2.4×10^{11}	7.7×10^{4}
	Medium[b]	1.4×10^{12}	1.9×10^{4}
	Small[b]	5.3×10^{12}	1.0×10^{4}
NPs-Ru(bpy)$_2$bps	**Large**[a]	3.0×10^{11}	3.4×10^{4}
	Medium[b]	5.8×10^{11}	2.3×10^{4}
	Small[b]	3.7×10^{13}	7.3×10^{2}

8. Confocal luminescence microscopy and confocal image analysis. Confocal images were acquired with a Nikon A1R microscope served by NIS-Elements Version D 3.10 software (Nikon Instruments). An oil immersion objective with a high NA (NA = 1.45, magnification 100X), and a GaAsP PMT detector (HV = 135) were used during the measurements. The acquisition parameters were set to 1 A.U., 8X signal average, in Galvano scanning mode, with an excitation laser at 489 nm (laser power = 8.1%, and 525/50 nm and 595/50 nm emission filters). Settings were kept the same for all the samples that were analyzed. Images were acquired with a field of view of 45.95 x 45.95 µm^2 and a pixel size of 89.7 nm.

Image J software was used to analyze the recorded images. Images were 16-bit, with a resolution of 512x512 pixels and a pixel size of 89.7 nm. Images were stacks of a green channel image (emission filter 525/50 nm) and a red channel image (emission filter 595/50 nm). Upon elaboration, stack images were split into the green and the red channels separately. Only the red channel images, containing the luminescent signal in the range 570-620 nm were considered for the quantification of the Ru(II)-based dyes (Figure 7-ESI). All images were visualized with a brightness-to-contrast (B/C) range of 0-4096.

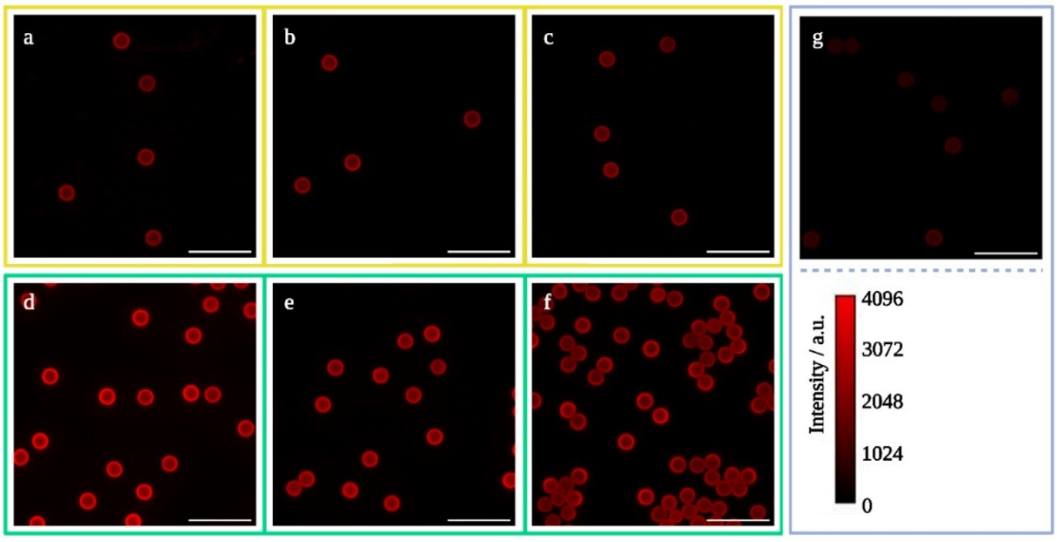

Figure 7-ESI a-c, yellow frame): red channel images of the photoluminescence acquired by confocal microscopy of 2.8 µm MMBs conjugated to **NPs-Ru(bpy)$_3^{2+}$** of *small, medium, and large* NPs respectively; **d-f** green frame): images for MMBs conjugated to **NPs-Ru(bpy)$_2$bps** of *small, medium, and large* NPs respectively. **g)** reference image for the unconjugated MMBs. Scale bar, 12 µm.

A squared area of 50x50 pixels centered on each bead was integrated to quantify the photoluminescence signal of DDSNP-conjugated beads. The same integration area was used to determine the background noise contribution to the luminescence. The average background noise (n=5) was subtracted from the signal of each bead. Then, the photoluminescence values of unconjugated microbeads - ascribable to residual polymer fluorescence - was subtracted to the values in the red channel of MMB@NPs, calculated in the same way, to finally obtain a net value of average intensity of Ru-probes in each microbead (Figure 8-ESI).

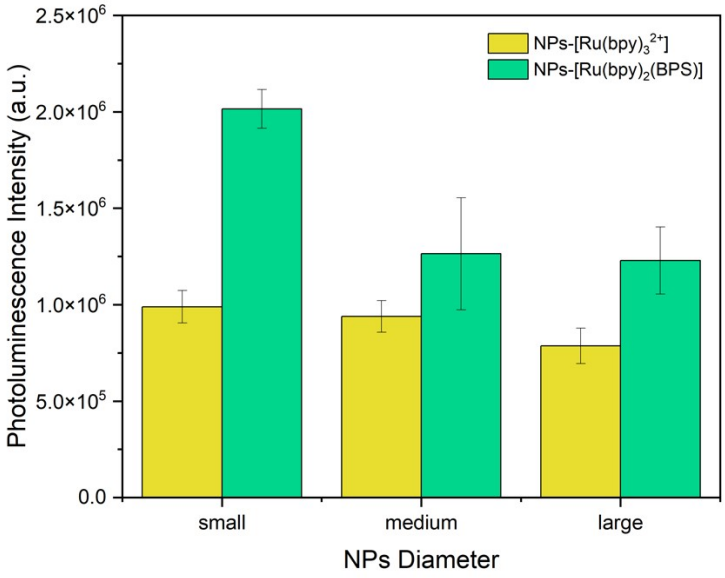

Figure 8-ESI photoluminescence intensities derived by confocal microscopy analysis of MMBs conjugated to *small, medium, and large* **NPs-Ru(bpy)$_3^{2+}$** (yellow); confocal photoluminescence intensities for MMBs conjugated to *small, medium, and large* NPs sizes **NPs-Ru(bpy)$_2$bps** (green). Error bars represent the standard error, n ≥ 3. Images were registered on a Nikon A1R microscope with an oil immersion, high NA objective (NA: 1.45, magnification 100×), an excitation laser at 489 nm, and a GaAsP PMT with an emission filter at 595/50 nm.

9. Single-bead ECL Microscopy. Measurements were carried out using a PTFE homemade electrochemical cell comprising a Pt working electrode (0.16 cm^2), a Pt counter electrode, and an Ag/AgCl (3M, KCl) reference electrode. For these measurements, an epifluorescence microscope (Nikon, Chiyoda, Tokyo, Japan) equipped with an ultrasensitive EMCCD camera (EM-CCD 9100−13, Hamamatsu, Japan - resolution of 512 × 512 pixels) was used. The microscope was equipped with a long-distance objective (100X, NA 0.80, W.D. 4.5 mm, Nikon, Chiyoda, Tokyo, Japan) and a motorized microscope stage (Corvus, Märzhauser, Wetzlar, Germany) allowing sample positioning. ECL image acquisition was triggered by a Biologic® SP300 potentiostat while applying a constant potential of 0 V for 2 seconds and 1.4V for 8 seconds (vs. Ag/AgCl 3M KCl). All the ECL microscopy images were acquired using the following parameters: sensitivity 1200, gain sensitivity 5, and exposure time 10s. The microscope was enclosed in a homemade dark box to avoid interferences from external light.

10. ECL emission mechanism

1) $TPrAH^+ \rightleftharpoons TPrA + H^+$

2) $TPrA - e^- \rightleftharpoons TPrA^{\bullet+}$

3) $TPrA^{\bullet+} \rightleftharpoons TPrA^{\bullet} + H^+$

4) $TPrA^{\bullet} + [\textbf{Ru-NP}]^n \rightarrow P1 + [\textbf{Ru-NP}]^{n-1}$

5) $TPrA^{\bullet+} + [\textbf{Ru-NP}]^{n-1} \rightleftharpoons TPrA + [\textbf{Ru-NP}]^{n*}$

6) [**Ru-NP**]^{n*} → [**Ru-NP**]^{n} + *hv*

Eqs. 1,6-ESI represent a plausible mechanism of the ECL emission for NPs in aqueous conditions under heterogeneous *oxidative-reduction* conditions, using TPrA as a co-reactant. **Ru-NP** represents **NPs-Ru(bpy)$_3^{2+}$** and **NPs-Ru(bpy)$_2$bps**.

11. ECL Images Analysis. The acquired images have been analyzed using the *Image J software*. All the images were 16-bit with a resolution of 512x512 pixels and a pixel size of 158.71 nm. Both optical and the corresponding ECL images were acquired (Figure 9-ESI). A squared area of 50x50 pixels centered on each bead was integrated to quantify the ECL signal of MMB@NPs (Figure 10-ESI). The same integration area has been used to determine the background noise contribution to the ECL. The average background noise (n=5) has been subtracted from the signal of each MMB@NPs.

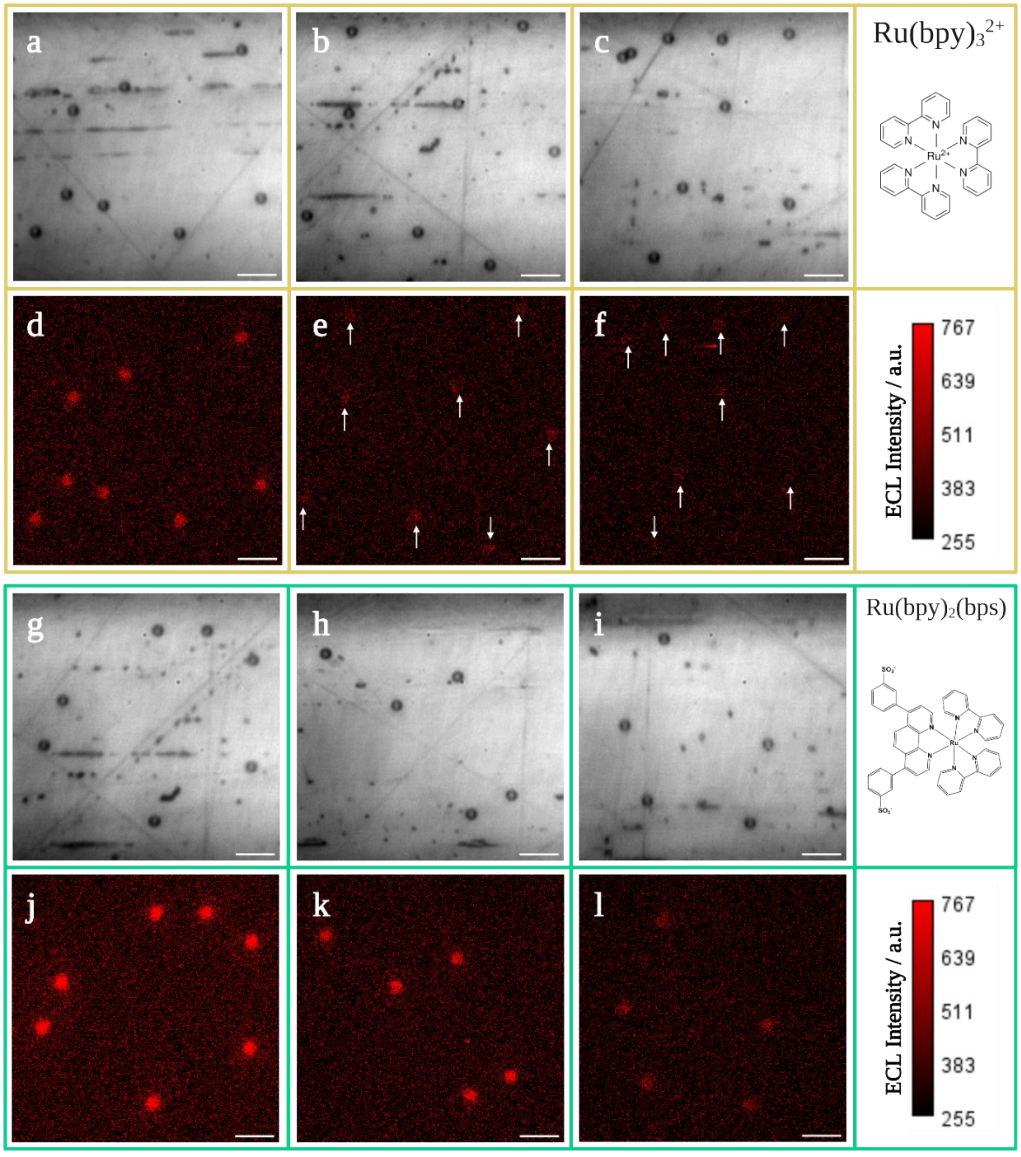

Figure 9 a-c) Optical and **d-f)** ECL images of 2.8 µm MMBs conjugated to **NPs-Ru(bpy)$_3^{2+}$** (top, yellow) of *small, medium, and large* size respectively. **g-i)** and **j-l)** are the analogue images with for **NPs-Ru(bpy)$_2$bps** (bottom, darker green frame) of *small, medium, and large* size respectively. The images have been acquired while applying a constant potential of 0 V for 2 s and of 1.4 V for 8 s (vs. Ag/AgCl) in 180 mM TPrA and 0.2 M phosphate buffer (PB) on a Pt working electrode and using a Pt wire as a counter electrode – integration time, 8 s; magnification, 100×; scale bar, 12 µm.

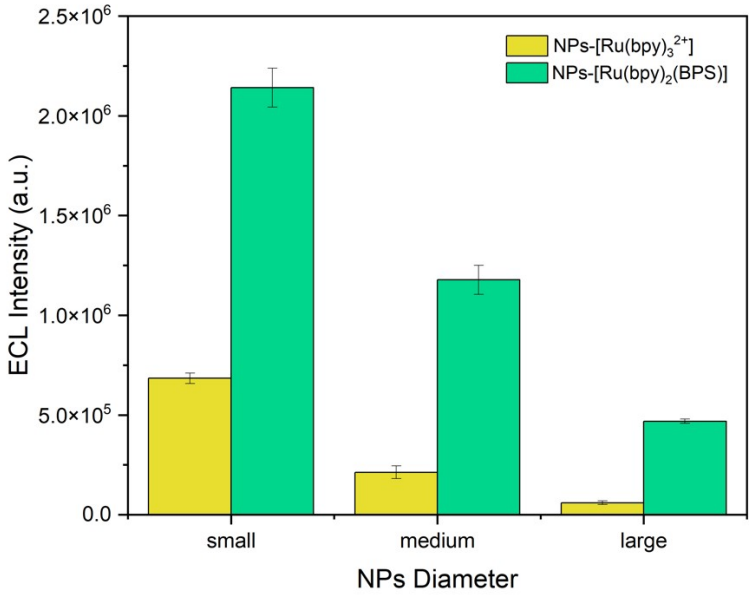

Figure 10-ESI ECL signal intensities of **NPs-Ru(bpy)$_3^{2+}$** of *small, medium, and large* size (yellow), and **NPs-Ru(bpy)$_2$bps** of small, medium, and large sizes (green). Error bars represent the standard error, n ≥ 3.

Finally, the ECL emission values of MMB@NPs were normalized by the luminescent signals of the same MMB@NPs determined by confocal microscopy (Figure 3 right).